Anionic and Neutral States of Li_3O

Maciej Gutowski† and Jack Simons*

Chemistry Department, University of Utah, Salt Lake City, Utah 84112

Received: January 14, 1994; In Final Form: May 27, 1994®

The ground state of the cation, three lowest electronic states of the neutral, and two anionic states of Li_3O were studied using different ab initio techniques. Stationary points on the potential energy surfaces were determined both at complete active space (CAS) self-consistent field (SCF) and at second-order Møller–Plesset (MP2) levels of theory. Excited states were approached using the single-excitation configuration interaction (CIS) method. Electron detachment energies for the anionic and neutral states were calculated at the quadratic configuration interaction (QCI) level with single, double, and approximate triple excitations (SD(T)) included. The calculations indicate that Li_3O^- possesses two bound electronic states. The ground $^1A_1'$ state has an equilibrium D_{3h} structure and a vertical electron detachment energy (VDE) of 0.66 eV. The $^3E'$ bound state pseudorotates through $^3A_1$ and $^3B_2$ stationary points. The barrier for pseudorotation was found to be less than 0.002 eV at the QCISD(T) level. Two VDE peaks for the $^3E'$ anion were predicted to be at 0.45 and 1.15 eV for transitions to the ground and the first excited state of the neutral, respectively. The ground state of the cation and the first three electronic states of the neutral Li_3O were also considered, and the vertical ionization potential for the ground neutral state was found to be 3.60 eV. Li_3O and Li_3O^- are thermodynamically stable with respect to the unimolecular decompositions Li_3O (neutral or anion) → Li_2O + Li (neutral or anion). Hence, the species should be amenable to experimental studies.

I. Introduction

Recent theoretical studies indicate that neutral molecular radicals containing alkali metal atoms can accommodate more than one bound anionic state. The simple alkali metal oxide diatomic molecules possess electronically bound anionic states of $^3\Pi$, $^1\Pi$, $^1\Sigma^+$, and $^3\Sigma^+$ symmetry.[1] Experimental[2,3] and theoretical[4] studies on alkali metal trimer anions (M_3^-) have concentrated primarily on the lowest $^1\Sigma_g^+$ isomer. Recently, we demonstrated that one triplet ($^3A_2'$) and two quintet ($^5A_1''$ and $^5A_2'$) states of Li_3^- and Na_3^- are also electronically stable for a wide range of molecular geometries.[5] Also, $LiFLi^-$ possesses two electronically bound states of $^1\Sigma_g^+$ and $^3\Sigma_u^+$ symmetry.[6]

The neutral Li_3O has already been studied both experimentally[7] and theoretically.[8-11] Wu et al. identified Li_3O by means of Knudsen effusion mass spectrometry in the vapor equilibrated with solid lithium oxide.[7] The values of the atomization energy and dissociation energy to produce Li + Li_2O were found to be 228.7 ± 2 and 50.7 ± 10 kcal/mol, respectively.[7,12] The ionization potential for Li_3O(g) of 4.54 ± 0.2 eV was evaluated by the extrapolated voltage difference method.[7]

Li_3O is an example of a "hypermetalated" molecule with a stoichiometry which violates the octet rule.[8] In addition, it is a promising candidate for being a "superalkali" (i.e., a molecular system whose first ionization potential is smaller than that of the Cs atom[9-11]). Both of these unusual chemical features are related to the nature of the highest occupied molecular orbital (HOMO). It displays bonding interactions between pairs of Li "ligands" which help to offset the octet-rule-violating structure and antibonding Li–O interactions.

Early predictions of a C_{2v} equilibrium structure for Li_3O[8] have not been confirmed in more advanced calculations[10,13] which indicated a D_{3h} structure, similar to that of Li_3O^+. Theoretical predictions of the adiabatic and vertical ionization potential produced 3.55 and 3.45 eV, respectively,[10,11] far outside the range of experimental values,[7] although the theoretical dissociation energy of 47.1 kcal/mol[10] agrees well with the experimental prediction.

To the best of our knowledge, neither the excited electronic states of the neutral nor the anionic states of Li_3O have yet been experimentally studied.

II. Computational Aspects

For the lithium atom, we used the Dunning (9s5p/3s2p) one-electron basis set[14] supplemented with diffuse s and p functions with the same exponent 0.0074[15] and one d function with the exponent 0.2.[16] This basis set is detailed in ref 5. For the oxygen atom we employed Dunning's aug-cc-pVDZ basis set which was designed to describe anionic species.[17] Cartesian d functions were used throughout the calculations, and the full basis set for the molecule consists of 82 contracted Gaussian functions.

Potential energy surfaces were explored within a complete active space (CAS) self-consistent-field (SCF) formalism as well as at the second-order Møller–Plesset (MP2) theory level.

In CAS SCF calculations we imposed a constraint that molecular orbitals which result from the core 1s atomic orbitals were doubly occupied in every configuration state function (CSF). The neglected core–core and core–valence correlation effects are negligible for the lithium and oxygen atoms due to the low polarizability of the 1s cores. The remaining eight (cation), nine (neutral), or ten (anion) electrons were distributed in all possible ways among four a_1, two b_1, and two b_2 molecular orbitals (the C_{2v} symmetry labeling is used). This choice of the active space led to 1764, 2352, 1176, and 1512 CSF's for the cation, neutral, singlet, and triplet anion, respectively. The CAS SCF calculations were performed with the Utah MESS-KIT modular electronic structure codes[18] which generate analytical second geometrical derivatives. Stationary points on the potential energy surfaces were determined using our automated surface walking algorithm.[19]

In the case of the neutral 2^2A_1 state, which correlates with the $^2E'$ state, the CAS SCF optimization was hindered by the problem of "root flipping".[20] Since the MP2 approach is inapplicable for excited electronic states, we invoked the single-excitation configuration interaction (CIS) approach[21] to determine geometry and relative energy of the 2^2A_1 transition state. The CIS results

* To whom correspondence should be addressed.
† Present address: IBM Research Division, Almaden Research Center, 650 Harry Road, San Jose, CA 95120-6099.
® Abstract published in *Advance ACS Abstracts*, July 15, 1994.

0022-3654/94/2098-8326$04.50/0

TABLE 1: Stationary Points (distances R in Å, Angles ϑ in deg) and Harmonic Frequencies (cm^{-1}) for Different Electronic States of the Cation, Neutral, and Anion of Li_3O[a]

species	symmetry	state	DEC	method	geometry	vibrational frequencies[b]	$\langle R^2 \rangle$	E_{QCI}
Li_3O^+	D_{3h}	$^1A_1'$	(+)	CAS	R = 1.726	a_2'' 244, e′ 265, a_1' 655, e′ 806	91	0.0
				MP2	R = 1.708	e′ 270 (73), a_2'' 291 (270), a_1' 687 (0), e′ 853 (290)		
Li_3O	D_{3h}	$^2A_1'$	(+)$4a_1'$	CAS	R = 1.707	e′ 251*i*, a_2'' 77, a_1' 669, e′ 767	141	–3.593
				MP2	R = 1.694	e′ 135 (462), a_2'' 180 (2), a_1' 699 (0), e′ 869 (109)		
Li_3O	D_{3h}	$^2E'$	(+)3e′	CAS	R = 1.696	not a stationary point	153	–2.856
Li_3O	C_{2v}	$^2B_2$	(+)$3b_2$	CAS	R_1 = 1.705	b_1 193, b_2 215, a_1 219, a_1 679, a_1 801, b_2 871	153	–2.890
					R_2 = 1.707			
					ϑ = 114.58			
				MP2	R_1 = 1.690	b_2 202 (9250), a_1 213 (87), b_1 243 (1), a_1 687 (52),		
					R_2 = 1.707	b_2 844 (148), a_1 849 (16)		
					ϑ = 114.96			
				CIS	R_1 = 1.662	b_1 210, b_2 229, a_1 244, a_1 697, b_2 814, a_1 903		
					R_2 = 1.699			
					ϑ = 117.96			
Li_3O	C_{2v}	2^2A_1	(+)$7a_1$	CIS	R_1 = 1.718	b_2 132*i*, b_1 211, a_1 424, a_1 702, b_2 745, a_1 1025		–2.854[c]
					R_2 = 1.671			
					ϑ = 121.08			
Li_3O	D_{3h}	$^2A_2''$	(+)$2a_2''$	CAS	R = 1.706	a_2'' 215, e′ 232, a_1' 678, e′ 804	189	–2.042
				MP2	R = 1.697	e′ 232 (403), a_2'' 247 (4), a_1' 702 (0), e′ 839 (1353)		
Li_3O^-	D_{3h}	$^1A_1'$	(+)$4a_1'^2$	CAS	R = 1.708	a_2'' 85, e′ 180, a_1' 666, e′ 748	274	–4.248
				MP2	R = 1.697	e′ 171 (77), a_2'' 172 (179), a_1' 693 (0), e′ 856 (214)		
Li_3O^-	D_{3h}	$^3E'$	(+)$4a_1'3e'$	CAS	R = 1.693	not a stationary point	254	–3.960
Li_3O^-	C_{2v}	$^3A_1$	(+)$6a_1 7a_1$	CAS	R_1 = 1.709	b_2 144, b_1 149, a_1 257, a_1 673, b_2 723, a_1 858	249	–4.023
					R_2 = 1.707			
					ϑ = 131.18			
				MP2	R_1 = 1.717	b_2 101 (123), b_1 202 (166), a_1 235 (316), a_1 682 (5),		
					R_2 = 1.697	b_2 806 (781), a_1 875 (458)		
					ϑ = 129.23			
Li_3O^-	C_{2v}	$^3B_2$	(+)$6a_1 3b_2$	CAS	R_1 = 1.700	b_2 270*i*, b_1 144, a_1 191, a_1 673, a_1 761, b_2 809	246	–4.024
					R_2 = 1.707			
					ϑ = 109.43			
				MP2	R_1 = 1.692	b_2 154*i* (6108), a_1 176 (342), b_1 200 (162),		
					R_2 = 1.709	a_1 682 (139), a_1 824 (439), b_2 845 (318)		
					ϑ = 109.81			

[a] The lowest-energy D_{3h} structures for the $^2E'$ and $^3E'$ states are also presented. The spatial extent of the SCF electronic charge distribution $\langle R^2 \rangle$ is given in au, and the relative energies (QCISD(T) level) are in eV. The dominant electronic configurations (DEC) are given with respect to the closed-shell cationic core $3a_1'^2 2e'^2 1a_2''^2$, which is denoted (+). [b] IR intensities (km/mol) in parentheses. [c] The energy of 2^2A_1 is estimated as $E_{QCI}(^2B_2) + E_{CIS}(2^2A_1) - E_{CIS}(^2B_2)$.

for the doublet neutral state should be considered cautiously. In the CIS approach, creation of spin eigenstates relies on having an RHF ground state and noninteraction of singlets and triplets does not carry over to doublets and quartets with a UHF reference. The Gaussian 92 code[22] attempts to handle these doublet cases, but the theory is not clean anymore.[23] In view of the above doubts, we "calibrated" the CIS approach on the $^2B_2$ electronic state which also correlates with $^2E'$ but for which the CAS SCF and MP2 approaches are straightforwardly applicable.

In the MP2 geometry optimizations we allowed for the correlation of the core orbitals. In general, the structures corresponding to stationary points are quite similar at the CAS SCF and MP2 levels, which suggests that the core–core and core–valence correlation effects are not important for geometrical predictions.

The restricted CAS SCF approach is capable to predict accurate geometries, but it is inappropriate to accurately compare energies of species with a different number of electrons. Hence, we employed the quadratic configuration interaction (QCI) approach with single, double, and approximate triple excitations (SD(T))[24] to determine relative energies and electron detachment energies. The QCISD(T) approach is size-extensive and takes into account dynamical correlation effects. In the QCI calculations, we kept the eight core electrons uncorrelated. We checked in our earlier study on $LiFLi^-$[6] that such a restriction changes in the vertical detachment energy for the ground-state anion by less than 0.003 eV. The QCI results were obtained with the Gaussian 92 suite of codes.[22]

III. Results

The stationary points on the potential energy surfaces of the cation, neutral, and anion determined at the CAS SCF and MP2 levels are characterized in Table 1, and the geometrical parameters used are defined in Figure 1. The vibrational frequencies were calculated using analytical second derivatives. For the excited $^2B_2$ and 2^2A_1 states of the neutral, stationary points are also reported at the CIS level. The spatial extents of the electronic charge distributions are characterized by the SCF values of $\langle R^2 \rangle$. The relative energies were obtained at the QCISD(T) level, as were our vertical detachment energies (VDE) and adiabatic electron affinities (EA_a) presented in Tables 2 and 3 for the neutral and the anion, respectively. The relative energies of various electronic states for the neutral and the anion are schematically presented in Figure 2.

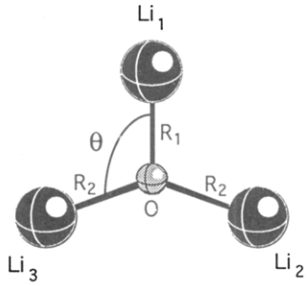

Figure 1. Geometrical parameters for the C_{2v} structure of the Li_3O neutral and anionic species.

A. The Cation and Neutral. The D_{3h} electronic configuration for the closed-shell *cation* involves an orbital occupation $3a_1'^2 2e'^2 1a_2''^2$ (the core 1s orbitals are not included in this labeling) which will be denoted (+). Our D_{3h} geometry and frequencies for the closed-shell cation are quite similar at the CAS SCF and MP2 levels. They are also in good agreement with the results of Rehm et al.[10] The pyramidization mode (a_2''),

TABLE 2: Vertical Electron Ionization Potentials (VIP) and Adiabatic Ionization (IPa) (in eV) Calculated at the QCISD(T) Level for $Li_3O^+ + e^- \leftarrow Li_3O$

transition	VIP	IP_a
$^1A_1' + e^- \leftarrow {}^2A_1'$	3.603	3.593
$^1A_1 + e^- \leftarrow {}^2B_2$	2.933	2.890
$^1A_1 + e^- \leftarrow 2^2A_1$[a]	2.954	2.909
$^1A_1' + e^- \leftarrow {}^2A_2''$	2.052	2.042

[a] The energy of 2^2A_1 is estimated as in Table 1.

TABLE 3: Vertical Electron Detachment Energies (VDE) and Adiabatic Electron Affinities (EA_a) (in eV) Calculated at the QCISD(T) Level for $Li_3O + e^- \leftarrow Li_3O^-$

transition	VDE	EA_a
$^2A_1' + e^- \leftarrow {}^1A_1'$	0.656	0.656
$1^2A_1 + e^- \leftarrow {}^3A_1$	0.450	0.430
$2^2A_1 + e^- \leftarrow {}^3A_1$	1.346[a]	1.074[b]
$1^2A_1 + e^- \leftarrow {}^3B_2$	0.459	0.431
$^2B_2 + e^- \leftarrow {}^3B_2$	1.151	1.134

[a] The VDE is estimated as $E_{QCI}(^3A_1) - E_{QCI}(^2B_2) + E_{CIS}(^2B_2) - E_{CIS}(2^2A_1)$. [b] The EA_a is estimated as VDE + $E_{CIS}(2^2A_1$ at the $^3A_1$ geometry) − $E_{CIS}(2^2A_1$ at its CIS stationary point).

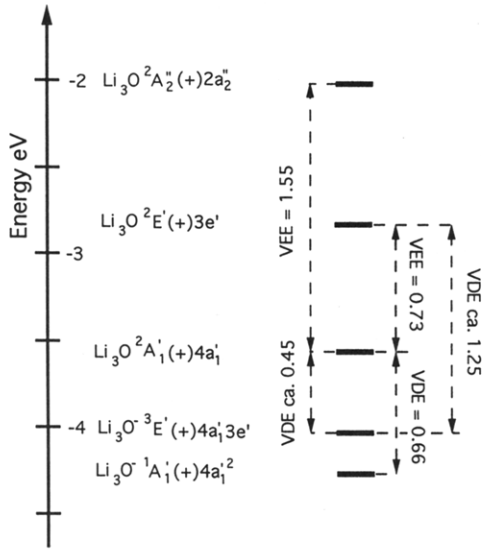

Figure 2. Relative energies (in eV) of the low-lying electronic states for the states of neutral and anionic Li_3O measured with respect to the ground state D_{3h} cation. Vertical electron detachment energies (VDE) for the anionic states and the vertical excitation energies (VEE) for the ground-state neutral are also marked.

which lowers symmetry to C_{3v}, has the lowest frequency. Interestingly, the cation H_3O^+, studied earlier,[25] has a C_{3v} equilibrium structure with the D_{3h} barrier of only 1.07 kcal/mol.[26]

The MP2 equilibrium structure of the ground-state *neutral* with the electronic configuration $(+)4a_1'$ is again D_{3h} and similar to that of the cation. Because the $^2A_1'$ wave function is found to have a single-configuration character, the MP2 prediction should be quite accurate. Unexpectedly, the e′ (in-plane) vibrational mode has an imaginary frequency at the CAS SCF level. Doubting whether the CAS SCF e′ imaginary frequency is physically meaningful, we carried out a CAS SCF search for a new stationary point in C_{2v} symmetry and found a structure with $R_1 = 1.683$ Å, $R_2 = 1.731$ Å, $\vartheta = 133°$, and an energy 0.06 eV lower than at the D_{3h} stationary point. However, the QCISD(T) energy is lower by 0.02 eV at the D_{3h} than at the C_{2v} CAS SCF stationary point. Hence, we conclude that the D_{3h} structure corresponds to a genuine minimum, and the CAS SCF approach suffers for symmetry-breaking artifacts.[27] Even though this $^2A_1'$ state has a D_{3h} equilibrium structure, the MP2 vibrational frequencies of the a_2'' and e′ modes are much softer than in the

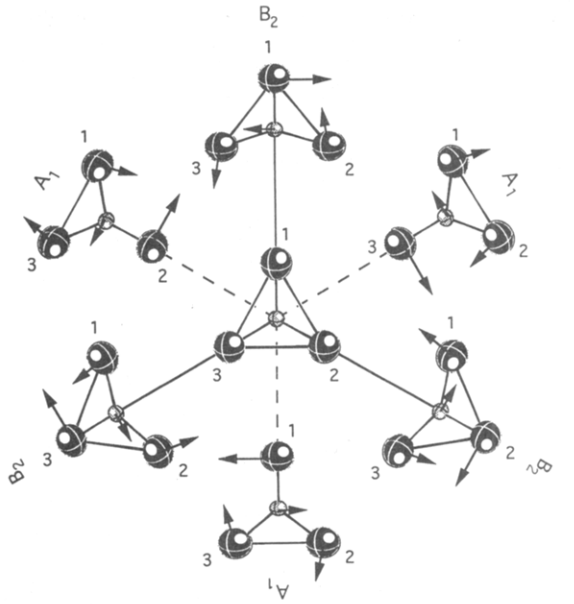

Figure 3. Graph representing the pseudorotation for the triplet (anion) or doublet (neutral) E′ states. Along the solid lines are the C_{2v} structures with $\theta < 120°$ (B_2 electronic states). Along the dashed lines are the C_{2v} structures with $\theta > 120°$ (A_1 electronic states). The intermediate structures have C_s symmetry.

underlying cation which implies that C_{3v}, C_{2v}, and C_s symmetries are easily accessible by vibrational movement.

The $4a_1'$ HOMO of the neutral is dominated by Li 2s orbitals which interact constructively with each other and destructively with small s-type contributions from the central O atom, as observed in refs 8–10. The Mulliken population atomic charges are +0.20 and −0.60 for Li and O, respectively. Our values for the vertical and adiabatic ionization potentials ($Li_3O(^2A_1') \rightarrow Li_3O^+(^1A_2') + e^-$) are VIP = 3.60 and IP_a = 3.59 eV, respectively, in good agreement with the electron propagator theory VIP of 3.45 eV.[11] However, these results disagree with the experimental estimation of 4.54 ± 0.2 eV.[7] The theoretical VIP for Li_3O is lower than that of alkali metal atoms, so our result support the claimed "superalkali" nature of Li_3O.[9-11]

The first *excited* state for the neutral of $^2E'$ symmetry has a dominant orbital occupancy of (+)3e′ and is subject to first-order Jahn–Teller (FOJT) distortion. Geometry optimization for the resulting $^2B_2$ component of this state is straightforward, and the resulting CAS SCF and MP2 geometries and frequencies are quite similar. Due to problems with "root flipping" at the CAS SCF level, geometry optimization for the 2^2A_1 component of this $^2E'$ state was performed at the CIS level. The reliability of the CIS approach was tested on the $^2B_2$ state where the stationary point characteristics were found to be similar for the CIS, CAS SCF, and MP2 approaches. We therefore believe that application of the CIS approach to the 2^2A_1 state is justified.

The C_{2v} structures of the $^2B_2$ and $^2A_1$ stationary points are determined by the nature of the singly occupied orbitals: $3b_2$ and $7a_1$, respectively. The $3b_2$ orbital is dominated by the s- and p-type atomic orbitals of $Li_{(2)}$ and $Li_{(3)}$. Due to the $Li_{(2)}$–$Li_{(3)}$ interaction dictated by the b_2 symmetry, the equilibrium $^2B_2$ structure has $\theta < 120°$ and $R_1 < R_2$. On the other hand, for the $7a_1$ orbital the interactions between s- and p-type AO of Li_2 and Li_3 are constructive by symmetry, and the $Li_1 + Li_{2(3)}$ interactions are destructive. These two features lead to $\theta > 120°$ and $R_1 > R_2$ for the $^2A_1$ stationary point.

Pseudorotation in the $^2E'$ state is depicted in Figure 3. The $^2B_2$ and $^2A_1$ stationary points are connected by a C_s symmetry reaction path. The energy difference between the lowest energy D_{3h} structure of $^2E'$ symmetry specified in Table 1 and the $^2B_2$ minimum is 0.03 eV. Estimating the pseudorotation barrier requires a consistent calculation of the 2^2A_1 and $^2B_2$ energies. An

estimate for the 2^2A_1 energy was obtained within the approximation $E(2^2A_1) \cong E_{QCI}(^2B_2) - E_{CIS}(^2B_2) + E_{CIS}(2^2A_1)$, because only the CIS method could be applied directly to the 2^2A_1 state. The barrier for pseudorotation thus found is 0.04 eV.

The CIS oscillator strength for the $^2E' \leftarrow {}^2A_1'$ transition is 0.48, and the QCISD(T) vertical excitation energy is 0.728 eV. Interestingly, the neutral $^2E'$ state thus produced would be in the neighborhood of its conical intersection. This fact could be reflected in the dynamics of the $^2E'$ state, which might be studied using time-dependent two-photon ionization techniques.[28]

The next excited state of Li_3O has $^2A_2''$ symmetry and (+)-$2a_2''$ orbital occupancy and an equilibrium D_{3h} structure. In comparison with the cation, the vibrational frequencies are quite similar and the equilibrium R is somewhat shorter. These features are consistent with the "out-of-plane" nature of the $2a_2''$ orbital, and similar trends were observed in the alkali metal trimers with the unpaired electron in an a_2'' orbital.[5,29] In Li_3O, the $2a_2''$ orbital is dominated by the Li 2p atomic orbitals with constructive Li–Li and destructive Li–O interactions. The CIS oscillator strength for the $^2A_2'' \leftarrow {}^2A_1'$ transition is 0.32, and the QCISD-(T) vertical excitation energy is 1.551 eV.

B. The Anion. The ground electronic state of Li_3O^- has a D_{3h} equilibrium structure with a geometry close to that of the cation and that of the ground-state neutral. There is a significant difference between the a_2'' out-of-plane vibrational frequency calculated at the MP2 and CAS SCF levels, but both approaches predict a D_{3h} minimum. The MP2 frequencies are quite similar for the anion and the $^2A_1'$ neutral.

The wave function for the anionic $^1A_1'$ state is dominated by the $(+)4a_1'^2$ configuration, but two equivalent contributions from the $(+)3e'^2$ configuration are also important and have CI coefficients of 0.30 each. This feature is consistent with the low separation between the $^2A_1'$ and $^2E'$ states of the neutral (0.7 eV) and suggests that $^3E'$ anionic state may be also electronically stable. The VDE for the $^1A_1'$ anion state is 0.656 eV, and the electron detachment peak is expected to be sharp because the anion and neutral equilibrium structures are very similar.

In addition to the ground $^1A_1'$ state, Li_3O^- possesses a second electronically *bound* state of $^3E'$ symmetry with the dominant electronic configuration $(+)4a_1'3e'$. Due to FOJT distortion, stationary points develop on $^3B_2$ and $^3A_1$ surfaces. The structures of the anionic stationary points are determined by the nature of the second singly occupied orbital, i.e., $3b_2$ and $7a_1$ for the $^3B_2$ and $^3A_1$ states, respectively, and are analogous to the $^2E'$ neutral case discussed above. The energy difference between the lowest energy D_{3h} structure of $^3E'$ symmetry and the $^3B_2$ stationary point is 0.06 eV. Both CAS SCF and MP2 approaches locate a transition state on the $^3B_2$ surface with negative curvature along the b_2 distortion mode. The surface must, however, be extremely flat since, at the QCISD(T) level, the relative order of the $^3B_2$ and $^3A_1$ stationary points is changed, giving $^3B_2$ lower than $^3A_1$ by 0.001 eV, whereas the difference at the MP2 level is 0.011 eV with the opposite order. Clearly, the pseudorotation, as depicted in Figure 3, is practically free, and the calculated numerical values of the b_2 mode frequency are probably of little reliability.

The electron detachment energies for the pseudorotating $^3E'$ state were calculated at both daughter-state stationary points (see Table 3). The detachment energies to the ground $^2A_1'$ state of the neutral are predicted to lie in the range 0.43–0.46 eV. The detachment energies to the higher pseudorotating $^2E'$ state of the neutral lie within 1.1–1.4 eV. We thus conclude that the electron detachment peaks from the $^3E'$ anion state would bracket the anion's ground-state detachment peak at 0.66 eV. Hence, the $^3E'$ state may be amenable to experimental detection, providing a significant concentration of the triplet can be produced in the source.

Another feature which makes Li_3O and Li_3O^- suitable for experimental studies is their thermodynamic stability. The energy barriers (corrected for zero-point vibrations) for the decomposition of the cation, neutral, and anion ($Li_3O^{(+0-)} \rightarrow Li_2O + Li^{(+0-)}$) are predicted to be 84.40, 44.54, and 46.03 kcal/mol, respectively. The increased stability of the anion compared to that of the neutral reflects the fact that the electron affinity is larger for Li_3O than for Li. Our decomposition energy for the neutral is within the range of experimental data, 50.7 ± 10 kcal/mol.[7,12]

IV. Conclusions

Theoretical calculations indicate that Li_3O^- can possess more than one bound electronic state. The fully symmetric singlet state is the ground state, but the pseudorotating $^3E'$ state is also electronically bound.

For the ground $^1A_1'$ state of Li_3O^-, the electron detachment energy is 0.66 eV. The cation, ground-state neutral, and the anion all have equilibrium D_{3h} geometries, with the O–Li distances in the range 1.71–1.69 Å (at the MP2 level).

The pseudorotating *anionic* $^3E'$ state is electronically stable with respect to the $^2A_1'$ and $^2E'$ states of the neutral by ca. 0.4 and 1.1 eV, respectively. The geometrical features of the daughter-state $^3A_1$ and $^3B_2$ stationary points are consistent with the bonding or antibonding interactions among the atomic orbitals contributing to the respective anion state's singly occupied molecular orbitals. The QCISD(T) energies of these two stationary points are the same to within 0.002 eV. Hence, the pseudorotation is practically free.

For the neutral Li_3O, we studied the $^2E'$ and $^2A_2''$ excited states in addition to the $^2A_1'$ ground state. The $^2E'$ state pseudorotates through a $^2B_2$ minimum and a 2^2A_1 transition state with a pseudorotation barrier less than 0.03 eV. The oscillator strength for the $^2E' \leftarrow {}^2A_1'$ transition is 0.48, and the corresponding vertical excitation energy is 0.728 eV.

The $^2A_2''$ neutral, with a D_{3h} equilibrium structure, is separated from the ground-state neutral by 1.551 eV and is easily accessible since the oscillator strength is 0.32.

Our vertical and adiabatic ionization potentials for Li_3O of 3.60 and 3.59 eV, respectively, disagree with the experimental value of 4.54 ± 0.2 eV,[7] yet agree with other theoretical predictions.[10,11]

All of the species discussed in this study are thermodynamically stable with respect to unimolecular decomposition. Hence, the neutral and the anion are more amenable to experimental studies than their hydrogen-substituted analogs H_3O and H_3O^-, which are thermodynamically unstable.[25]

An ability to accommodate two bound anionic states is shared not only by LiFLi and Li_3O but also by the isoelectronic Li_4N. Our preliminary results for Li_4N^- produce a VDE from the $^1A_1$ state of ca. 0.51 eV. For the $^3T_2$ state of Li_4N^-, the VDE is ca. 0.17 eV, whereas detachment to the $^2T_2$ state of the neutral Li_4N would require ca. 0.98 eV.

Acknowledgment. This work was supported by the Office of Naval Research and National Science Foundation Grant CHE9116286.

References and Notes

(1) Bauschlicher, Jr., C. W.; Partridge, H.; Pettersson, L. G. M. *J. Chem. Phys.* **1993**, *99*, 3654.
(2) McHugh, K. M.; Eaton, J. G.; Lee, G. H.; Sarkas, H. W.; Kidder, L. H.; Snodgrass, J. T.; Manaa, M. R.; Bowen, K. H. *J. Chem. Phys.* **1989**, *91*, 3792. Bowen, K. H.; Eaton, J. G. In *The Structure of Small Molecules and Clusters*; Naaman, R., Vager, Z., Eds.; Plenum Press: New York, 1988.
(3) Sarkas, H. W.; Arnold, S. T.; Hendricks, J. H.; Bowen, K. H. Manuscript in preparation.
(4) Bonacic-Koutecky, V.; Fantucci, P.; Koutecky, J. *Chem. Rev.* **1991**, *91*, 1035.
(5) Gutowski, M.; Simons, J. *J. Chem. Phys.*, in press.
(6) Gutowski, M.; Simons, J. *J. Chem. Phys.* **1994**, *100*, 1308.
(7) Wu, C. H.; Kudo, H.; Ihle, H. R. *J. Chem. Phys.* **1979**, *70*, 1815.
(8) Schleyer, P. v. R.; Wurthwein, E.-U.; Pople, J. A. *J. Am. Chem. Soc.* **1982**, *104*, 5839.

(9) Gutsev, G. L.; Boldyrev, A. I. *Chem. Phys. Lett.* **1982**, *92*, 262.
(10) Rehm, E.; Boldyrev, A. I.; Schleyer, P. v. R. *Inorg. Chem.* **1992**, *31*, 4834.
(11) Zakrzewski, V. G.; von Niessen, W.; Boldyrev, A. I.; Schleyer, P. v. R. *Chem. Phys. Lett.* **1992**, *197*, 195.
(12) Kudo, H.; Wu, C. H. *Chem. Express* **1990**, *5*, 633.
(13) Wurthwein, E.-U.; Schleyer, P. v. R.; Pople, J. A. *J. Am. Chem. Soc.* **1984**, *106*, 6973.
(14) Dunning, Jr., T. H. Unpublished results.
(15) Clark, T.; Chandrasekhar, J.; Spitznagel, G.; van Rague Schleyer, P. *J. Comput. Chem.* **1982**, *4*, 294.
(16) Binkley, J. S.; Pople, J. A. *J. Chem. Phys.* **1977**, *66*, 879.
(17) Woon, D. E.; Dunning, Jr., T. H. *J. Chem. Phys.* **1993**, *98*, 1358.
(18) The Utah MESS-KIT is a suite of highly modular codes that were programmed in-house to give a variety of electronic structure functionalities by J. A. Nichols, M. R. Hoffmann, R. A. Kendall, H. L. Taylor, D. W. O'Neal, E. Earl, R. Hernandez, M. Gutowski, J. Boatz, K. Bak, J. Anchell, X. Wang, M. Feyereisen, and J. Simons.
(19) Nichols, J.; Taylor, H.; Schmidt, P.; Simons, J. *J. Chem. Phys.* **1990**, *92*, 340. Simons, J.; Jørgensen, P.; Taylor, H.; Ozment, J. *J. Phys. Chem.* **1983**, *87*, 2745. O'Neal, D.; Taylor, H.; Simons, J. *J. Phys. Chem.* **1984**, *88*, 1510. Banerjee, A.; Adams, N.; Simons, J.; Shepard, R. *J. Phys. Chem.* **1985**, *89*, 52. Taylor, H.; Simons, J. *J. Phys. Chem.* **1985**, *89*, 684. Cerjan, C. J.; Miller, W. H. *J. Chem. Phys.* **1981**, *75*, 2800. Baker, J. *J. Comput. Chem.* **1988**, *9*, 465. Baker, J. *J. Comput. Chem.* **1986**, *7*, 385.
(20) Olsen, J.; Jorgensen, P.; Yeager, D. L. *J. Chem. Phys.* **1982**, *76*, 527.
(21) Foresman, J. B.; Head-Gordon, M.; Pople, J. A.; Frisch, M. J. *J. Phys. Chem.* **1992**, *96*, 135.
(22) Gaussian 92, Revision A: Frisch, M. J.; Trucks, G. W.; Head-Gordon, M.; Gill, P. M.; Wong, M. W.; Foresman, J. B.; Johnson, B. G.; Schlegel, H. B.; Robb, M. A.; Replogle, E. S.; Gomperts, R.; Andres, J. L.; Raghavachari, K.; Binkley, J. S.; Gonzales, C.; Martin, R. L.; Fox, D. J.; DeFrees, D. J.; Baker, J.; Stewart, J. J. P.; Pople, J. A. Gaussian Inc., Pittsburgh, PA, 1992.
(23) Fox, D. J. Private communication.
(24) Pople, J. A.; Head-Gordon, M.; Raghavachari, K. *J. Chem. Phys.* **1987**, *87*, 5968.
(25) Ortiz, J. V. *J. Chem. Phys.* **1989**, *91*, 7024. Gutowski, M.; Simons, J. *J. Chem. Phys.* **1990**, *93*, 3874. Simons, J.; Gutowski, M. *Chem. Rev.* **1991**, *91*, 669.
(26) Colvin, M. E.; Raine, G. P.; Schaefer, H. F.; Dupuis, M. *J. Chem. Phys.* **1983**, *79*, 1551.
(27) Allen, W. D.; Horner, D. A.; Dekock, R. L.; Remington, R. B. *Mol. Phys.* **1989**, *133*, 11. van Lenthe, J. H.; van Duijneveldt, F. B. *J. Chem. Phys.* **1984**, *81*, 3168. Davidson, E. R.; Borden, W. T. *J. Phys. Chem.* **1983**, *87*, 4783.
(28) Gaus, J.; Kobe, K.; Bonacic-Koutecky, V.; Huhling, H.; Manz, J.; Reischl, B.; Rutz, S.; Schreiber, E.; Woste, L. *J. Phys. Chem.* **1993**, *97*, 12509.
(29) Gutowski, M.; Simons, J. Manuscript in preparation.